Variational Co-embedding Learning for Attributed Network Clustering

Shuiqiao Yang, Sunny Verma, Borui Cai, Jiaojiao Jiang, Kun Yu, Fang Chen, *Senior Member, IEEE* and Shui Yu, *Senior Member, IEEE*

Abstract—Recent works for attributed network clustering utilize graph convolution to obtain node embeddings and simultaneously perform clustering assignments on the embedding space. It is effective since graph convolution combines the structural and attributive information for node embedding learning. However, a major limitation of such works is that the graph convolution only incorporates the attribute information from the local neighborhood of nodes but fails to exploit the mutual affinities between nodes and attributes. In this regard, we propose a variational co-embedding learning model for attributed network clustering (VCLANC). VCLANC is composed of dual variational auto-encoders to simultaneously embed nodes and attributes. Relying on this, the mutual affinity information between nodes and attributes could be reconstructed from the embedding space and served as extra self-supervised knowledge for representation learning. At the same time, trainable Gaussian mixture model is used as priors to infer the node clustering assignments. To strengthen the performance of the inferred clusters, we use a mutual distance loss on the centers of the Gaussian priors and a clustering assignment hardening loss on the node embeddings. Experimental results on four real-world attributed network datasets demonstrate the effectiveness of the proposed VCLANC for attributed network clustering.

Index Terms—Attributed network clustering, graph convolutional neural network, variational auto-encoder.

arXiv:2104.07295v1 [cs.LG] 15 Apr 2021

1 Introduction

Finding accurate communities or clusters in an attributed network is critical to understand the complex network structures for many downstream applications like group recommendation, user-targeted online advertising, and disease protein discovery [1], [2], [3]. Though the clustering for attributed network brings many important applications, but it also poses significant new challenges. Firstly, as the attributed network includes not only structural connections but also attribute values, it is difficult to naturally combine and leverage the two types of information in the process of clustering [4]. Furthermore, it is usually hard to find supervision information to guide the cluster discovery in attributed network [5], [6], [7], [8].

To handle the challenges, many network embedding and graph neural network related methods have been developed recently for node representation learning to improve the accuracy of downstream applications like graph classification, link prediction and graph clustering. The representative methods include DeepWalk [9], Line [10], node2vec [11], struc2vec [12], GCN [13], GraphSAGE [14], ARGA/ARVGA [15], MGAE [16], AGC [8], etc. For example, DeepWalk [9] and Node2Vec [11] are two representative network embedding methods to learn low-dimensional representations for nodes through the local neighborhood structure prediction. Then, general clustering algorithms such as K-means can be adopted on the learned node embeddings for the network clustering task. Similarly, the graph convolutional network (GCN) proposed by Kipf *et al*. has also been widely exploited into the graph clustering task [13]. For example, AGC exploits a K-order GCN to update the features of each node via the k-hop neighbors and then adopts spectral clustering to find the best node partitions based on the new features for each node. These decoupled clustering strategies show great improvement in network clustering due to the improved node representations. However, they are sub-optimal in nature as the node representation learning process are independent with the node clustering process.

Later, graph auto-encoder based framework with self-contained clustering strategies have been proposed for attributed network clustering to overcome the aforementioned drawbacks. The methods include VGAECD [17], DAEGC [7], NEC [5], SDCN [6], etc. In these methods, graph neural network is used as the encoder and inner product between latent variables would be the decoder to reconstruct the input data for self-supervised learning [18]. A clustering objective is jointly optimized with the reconstruction loss to learn node embeddings that are optimal for clustering purpose. For example, VGAECD [17] finds the community structure by jointly optimizing a variational auto-encoder (VAE) and a Gaussian mixture model. NEC [5] jointly learns the node embedding and node community assignments by adding a soft clustering loss and modularity loss into the graph auto-encoder framework. SDCN [6] integrates the structural information for clustering using a DNN module and a GCN module to learn different aspects of information, and adopts a dual self-supervised mechanism to unify the learned representation from the two modules.

However, these methods only aggregate the attributes from the local neighborhood for node representation learning but ignore the mutual affinity information between nodes and

- *S. Yang, S. Verma, K. Yu and F. Chen are with Data Science Institute, University of Technology Sydney, Ultimo NSW 2007, Australia. E-mails: shuiqiao.yang@uts.edu.au, sunny.verma@uts.edu.au, kun.yu@uts.edu.au, fang.chen@uts.edu.au.*
- *B. Cai is with School of Information Technology, Deakin University, Burwood VIC 3125, Australia. E-mail: b.cai@deakin.edu.au.*
- *J. Jiang is with School of Computer Science and Engineering, University of New South Wales, Sydney NSW 2052, Australia. E-mail: jiaojiao.jiang@unsw.edu.au.*
- *S. Yu is with the School of Computer Science, University of Technology Sydney, Ultimo NSW 2007, Australia. E-mail: shui.yu@uts.edu.au.*

Manuscript is under review.

attributes. But mutual affinities between nodes and attributes such that a node contains different attributes and the same attribute could be shared by different nodes can denote much deep and implicit information. For example, much fine-grained node similarities at attribute level could be retained given the affinities from nodes to attributes. Therefore, exploiting this affinities should be useful for learning better node representations. Moreover, these methods may not be able to learn more distinguishable representations due to the lack of separate prior distributions for different node clusters to regularize the node embedding learning.

To alleviate the aforementioned drawbacks, we propose a **V**ariational **C**o-embedding **L**earning model for **A**ttributed **N**etwork **C**lustering, abbreviated as VCLANC, which aims to embed the nodes and attributes into the same semantic space where the mutual affinities between nodes and attributes could be reconstructed for better representation learning. At the same time, we exploit a trainable Gaussian mixture model as priors on the latent variables to learn clustering friendly node embeddings and jointly infer the nodes clustering assignments. A mutual distance loss is deployed on the Gaussian priors to force different priors to become more separable. Also, a clustering assignment hardening loss is jointly optimized in the co-embedding learning process to further strength the clustering assignment qualities for the nodes.

Our contributions are summarized as follows:

I. We propose a variational co-embedding learning model named VCLANC for attributed network clustering. VCLANC exploits the mutual affinities between nodes and attributes as extra self-supervised knowledge to learn better node representations by using dual variational auto-encoders to co-embed nodes and attributes in the same latent space.
II. We simultaneously optimize trainable Gaussian mixture model with the dual variational auto-encoders in VCLANC to infer the clustering assignments in the embedding space. Meanwhile, we further adopt a mutual distance loss on Gaussian priors and a clustering assignment hardening loss on the node embedding space to strengthen the clustering effectiveness.
III. We conduct experiments on four real-world attributed network datasets to verify the effectiveness of VCLANC. The experimental results demonstrate the proposed method is more effective in the network clustering task and node embedding learning than the state-of-the-art methods.

The rest of this paper is organized as follows. Section 2 presents the related work. Section 3 introduces the notations, problem definition and preliminary. Section 4 details the proposed approach. Experimental setup is introduced in section 5. Experimental results are reported in section 6. Conclusions are made in section 7.

2 Related Work

We classify the related work for network clustering into two groups. The first group includes the traditional community detection related methods. The second group includes the deep learning based methods.

2.1 Community detection

For the non-attributed network, various methods have been developed to exploit the link structure of the networks to derive different connective patterns and partition the network into different communities. For example, the graph partitioning based methods iteratively divide the network until the stopping criteria is reached. For example, Kernighan *et al.* [19] have proposed a heuristic algorithm called Kernighan–Lin to randomly divide the network into two subsets and exchange the nodes between the subsets to find the optimal communities. The spectral clustering based methods have also been developed for community detection. For example, Donath *et al.* [20] have proposed to use the largest eigenvalues of the adjacent matrix for community detection. Shi *et al.* [21] have proposed the normalized spectral clustering method for community detection. Also, the modularity based methods have been proposed to find the optimal communities in network by maximizing the graph modularity [22], [23]. For example, Newman *et al.* [22] claim that the network modularity could be expressed as eigenvectors of a characteristic matrix. They first construct the modularity matrix for the target network and find the most positive eigenvalue with the associated eigenvector. Then, they divide the network into two parts based on the sighs of the elements in eigenvectors and repeat this process till the sub-networks are indivisible. Shang *et al.* [23] have proposed MIGA based on modularity and an improved genetic algorithm for community detection. They exploit the modularity as the objective function and the prior information of the community structures as target to make the community detection become more stable and accurate. The matrix factorization based methods focus on learning the main components to recover the adjacency matrix of a given network and thus reveal the network communities. Yang *et al.* [24] have proposed a method called BIGCLAM to find the overlapping communities through nonnegative matrix factorization.

Compared with the structure only non-attributed networks, the attributed networks with node features contain more comprehensive information. Hence, community detection in attributed networks has attracted much attention in recent years. For example, Neville *et al.* [25] define distance measurement between attributed nodes to weight the edges for better community detection. After that, the classical methods such as Karger's Min-Cut [26] and spectral clustering [27] are exploited on the weighted adjacent matrix to community detection or node clustering. Yang and Hong *et al.* [1], [28] have proposed SA-Cluster which first computes an augmented graph computed from the attribute information of nodes. Then, SA-Cluster exploits neighborhood random walk to compute a unified distance between vertices on using both the raw topological structure and augmented graph for community detection or node clustering. Combe [29] have adopted a hierarchical agglomerative clustering method based on a defined unified cosine distance on textual information of the nodes and geodesic distance on the network structure for community detection. Xu *et al.* [4] have proposed to integrate the structural and attribute information into a Bayesian model for clustering an attributed graph. In the Bayesian model, the clustering problem is transferred into a standard probabilistic inference problem, which is solved by a variational algorithm.

2.2 Deep learning for network clustering

To our best understanding, the methods for graph clustering via network embeddings or graph neural networks could be categorized into two types based on the different clustering strategies. In the first type, the methods focus on learning better

representations for nodes and then general clustering method like K-means is adopted for network clustering. For example, DeepWalk [9] learns the embedding for nodes through maximizing the probability of predicting its closest neighbors. The neighbors of a node are derived through random walk on the network structure. Node2Vec [11] make improvements for the node representation learning by optimizing a neighborhood preserving objective. The struc2vec [12] learns the node representation through a multilayer graph to encode structural similarities and structural context for nodes. Based on the improved representations of nodes, better network clustering performance could be reached using general clustering methods.

Later, graph convolutional network (GCN) is proposed and quickly becomes popular for graph data processing [13]. GCN creatively devises a graph convolution operation to aggregate the information from local neighborhood for node representation learning. Many variants have been proposed based on GCN. For example, GraphSAGE [14] improves GCN with trainable aggregator functions for better feature aggregation from the local neighborhood of nodes. Also, graph auto-encoder (GAE) and varitional graph auto-encoder (VGAE) have been proposed which using the GCN as encoder and the inner product between node embeddings as decoder in auto-encoder or variational auto-encoder framework for unsupervised representation learning [18], [30]. Based on GAE and VGAE, Pan *et al.* [15] have proposed ARGA and ARVGA with adversarial training scheme where the latent node representations are enforced to match a prior distribution. Wang *et al.* [16] have proposed MGAE which is a GAE with a marginalization process to disturb the network attribute information.

The second group of methods for graph clustering aim to jointly infer the clustering assignments and node embeddings. For example, Wang *et al.* [7] have proposed DAEGC, which exploits attentional strategy into GAE to determine the importance of neighboring nodes and uses a soft clustering loss as clustering objective to jointly infer the node clustering assignments. Sun *et al.* [5] have proposed NEC for attributed graph clustering using GAE with the same clustering objective in used DAEGC [7]. Additionally, NEC introduces a relaxed modularity loss to exploit the higher-order proximity of nodes for preserving community structure in the node representation learning. Bo *et al.* [6] have proposed SDCN which combines a DNN module, a GCN module, and a dual self-supervised module for comprehensive representation learning and graph clustering. Similarly, Li *et al.* [31] also have proposed DGSCN which combines both graph node feature and topology information with deep GCN layers and a triple self-supervised module for graph clustering. Choong *et al.* [17] have proposed VGAECD for attributed graph clustering. Unlike DAEGC and NEC, VGAECD exploits VGAE with a Gaussian mixture model based generative process to infer the clustering assignments.

3 Notations, Problem Definition and Preliminary

In this section, we introduce the mainly used notations and formally define the studied problem. After that, we introduce the preliminary for variational auto-encoder. The terms network and graph will be used interchangeably.

Table 1
Notations used in this paper.

Notation	Description
$\mathcal{G}$	attributed network
$\mathcal{V}$	node set
$\mathcal{A}$	attribute set
$\mathbf{A} \in \mathbb{R}^{N\times N}$	adjacency matrix for network
$\mathbf{X} \in \mathbb{R}^{N\times M}$	attribute matrix for nodes
$N = \lvert\mathcal{V}\rvert$	number of nodes
$M = \lvert\mathcal{A}\rvert$	number of attributes
J	dimension of latent variables
$\mathbf{Z}^{\mathcal{V}} \in \mathbb{R}^{N\times J}$	embedding matrix for the nodes
$\mathbf{Z}^{\mathcal{A}} \in \mathbb{R}^{M\times J}$	embedding matrix for the attributes

3.1 Notations

Table 1 summarizes the mainly adopted notations in this paper. An attributed network is denoted as $\mathcal{G}$ with four elements: the node set $\mathcal{V}$, the attribute set $\mathcal{A}$, the adjacent matrix $\mathbf{A}$ and the attribute matrix $\mathbf{X}$. $\mathcal{V}$ represents all the nodes in graph $\mathcal{G}$ and its size is $N = |\mathcal{V}|$. The structural connections of $\mathcal{G}$ are denoted with an adjacent matrix $\mathbf{A} \in \mathbb{R}^{N\times N}$ that is binary-valued (*i.e.*, zero or one) to represent the existence of edges between nodes, *e.g.*, $\mathbf{A}_{ij} = 1$ denotes that node i and node j have connection. The attributes of nodes in graph $\mathcal{G}$ are denoted as a matrix $\mathbf{X} \in \mathbb{R}^{N\times M}$, where the i^{th} row of $\mathbf{X}$ is represented with binary values which indicate the appearance of the raw attributes for i^{th} node in dimension size of M. Meanwhile, the j^{th} column of $\mathbf{X}$ denotes how the j^{th} attribute is distributed among different nodes. $\mathbf{A}$ represents the network structure and $\mathbf{X}$ represents the mutual affinities between nodes and attributes. The embeddings for nodes and attributes are denoted as $\mathbf{Z}^{\mathcal{V}} \in \mathbb{R}^{N\times J}$ and $\mathbf{Z}^{\mathcal{A}} \in \mathbb{R}^{N\times J}$, where the dimension size for the embedding space is J.

3.2 Problem Definition

With the adopted notations introduced above, we formally define the studied problem of attributed network clustering.

Definition 1 (Attributed network clustering). For a given attributed network $\mathcal{G} = (\mathcal{V}, \mathcal{A}, \mathbf{A}, \mathbf{X})$, the clustering for an attributed network is to find a partition function f that exploits the attribute matrix $\mathbf{X}$ and adjacent matrix $\mathbf{A}$ of $\mathcal{G}$ as inputs to divide the nodes $\mathcal{V}$ into disjoint sets in an unsupervised manner as follows:

$$(\mathbf{A}, \mathbf{X}) \xrightarrow{f} (\hat{\mathcal{V}}_1, \hat{\mathcal{V}}_2, \cdots, \hat{\mathcal{V}}_k), \tag{1}$$

such that: (1) the nodes with similar graph structure are more likely to be partitioned into the same set; (2) the nodes within a set are more likely to share similar attributes.

3.3 Preliminary for Variational Auto-encoder

The variational auto-encoder (VAE) is a self-supervised representation learning model which approximates the posterior distribution of latent variable and maximizes the marginal likelihood of the input data with an evidence lower-bound (*ELBO*) [30]. Fig. 1 shows the framework of the VAE model. For a given latent variable model $p_{\boldsymbol{\theta}}(\mathbf{X}, \mathbf{Z}) = p_{\boldsymbol{\theta}}(\mathbf{X}|\mathbf{Z})p(\mathbf{Z})$ where $\mathbf{X}$ denotes the observed data and $\mathbf{Z}$ denotes the latent representation, VAE uses an approximated posterior distribution $q_{\boldsymbol{\phi}}(\mathbf{Z}|\mathbf{X})$ for the intractable true posterior and then learns the optimal variational parameter $\boldsymbol{\phi}$ and the generative model

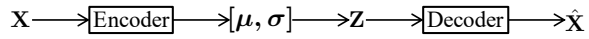


Figure 1. The framework of variational auto-encoder (VAE). Its encoder is an inference network which learns the latent representation for the inputs as Gaussian distributions. Its decoder is a generative network to reconstruct the input data.

parameters $\boldsymbol{\theta}$ through maximizing an evidence lower bound (*ELBO*) defined as follows:

$$\begin{aligned}\mathcal{L}_e(\boldsymbol{\theta}, \boldsymbol{\phi}; \mathbf{X}) =& \mathbb{E}_{q_{\boldsymbol{\phi}}}[\log p_{\boldsymbol{\theta}}(\mathbf{X}|\mathbf{Z})] - D_{KL}(q_{\boldsymbol{\phi}}(\mathbf{Z}|\mathbf{X}) \parallel p(\mathbf{Z})) \\ &\leq \log p(\mathbf{X}),\end{aligned} \tag{2}$$

where the posterior approximation distribution is generally a simple distribution such as a multivariate Gaussian distribution with diagonal covariance. $D_{KL}(q_{\boldsymbol{\phi}}(\mathbf{Z}|\mathbf{X}) \parallel p(\mathbf{Z}))$ is the Kullback-Leibler divergence (KL divergence) to measure the similarity between two probability distributions and it acts as a regularizer to force the posterior approximation distribution $q_{\boldsymbol{\phi}}(\mathbf{Z}|\mathbf{X})$ to be closer to the prior $p(\mathbf{Z})$.

As shown in Fig. 1, VAE is consisted with two computational networks: an *inference network* $f_{\boldsymbol{\phi}}(\cdot)$ called encoder and a *generative network* $g_{\boldsymbol{\theta}}(\cdot)$ called decoder. The inference network $f_{\boldsymbol{\phi}}(\cdot)$ is used to simulate the latent variable distribution $q_{\boldsymbol{\phi}}(\mathbf{Z}|\mathbf{X})$ while the generative network $g_{\boldsymbol{\theta}}$ is used to simulate $p_{\boldsymbol{\theta}}(\mathbf{X}|\mathbf{Z})$ to reversely generate the input data from the latent variables $\mathbf{Z}$. To learn the optimal representations for the raw data, VAE updates $f_{\boldsymbol{\phi}}(\cdot)$ and $g_{\boldsymbol{\theta}}(\cdot)$ simultaneously through optimizing the *ELBO* in Eq. 2. To generalize the training process of VAE, a reparameterization trick is adopted to exploit the general optimization methods like stochastic gradient descent [30]. The structures for $f_{\boldsymbol{\phi}}(\cdot)$ and $g_{\boldsymbol{\theta}}(\cdot)$ could be chose flexibly given different tasks. For instance, variational graph neural network (VGAE) [18] has been proposed to learn the embeddings for graph-structured data using graph convolutional neural network (GCN) [13] as the encoder.

4 Proposed Method

In this section, we elaborate our proposed method: variational co-embedding learning for attributed network clustering (VCLANC).

4.1 Overview of VCLANC

Fig. 2 shows the overall structure of VCLANC. VCLANC adopts dual variational auto-encoders to co-embed the nodes and attributes into the same latent space. A two-layer graph neural network (GCN) is used as an encoder to fuse the network topology $\mathbf{A}$ and the attribute matrix $\mathbf{X}$ for learning node embeddings $\mathbf{Z}^{\mathcal{V}}$. The inner product among $\mathbf{Z}^{\mathcal{V}}$ is used as the decoder to reconstruct the adjacent matrix as $\hat{\mathbf{A}}$. To exploit mutual affinities between nodes and attributes, VCLANC uses a two-layer multilayer perceptron (MLP) as encoder to embed the attributes of the network into the same latent space with nodes as $\mathbf{Z}^{\mathcal{A}}$ and then adopts the dot product between $\mathbf{Z}^{\mathcal{V}}$ and $\mathbf{Z}^{\mathcal{A}}$ as decoder to reconstruct the attribute matrix $\mathbf{X}$. The reconstructed $\hat{\mathbf{X}}$ and $\hat{\mathbf{A}}$ are used as self-supervised knowledge for optimizing the parameters of the dual variational auto-encoders.

To infer node clusters, we assume that the latent node embeddings of different groups follows Gaussian distributions

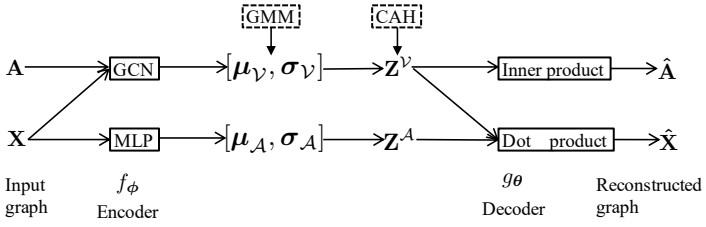


Figure 2. The structure of the proposed VCLANC model. A two-layer GCN and two-layer multilayer perceptron (MLP) are used as encoders to embed both nodes and attributes as Gaussian distributions with means and variances. Then, simple inner and dot product is used as encoders to reconstruct the input data. Trainable Gaussian mixture model (GMM) is used to infer the node clustering assignments and clustering assignment hardening (CAH) loss is adopted on node embeddings space to strengthen clustering quality.

as their priors. We incorporate the Gaussian mixture model (GMM) as priors to infer cluster assignments in the latent space. Meanwhile, a clustering assignment hardening (CAH) loss which adopts KL divergence to strengthen the confident nodes assignments from GMM is adopted to ensure better clustering qualities. We detail VCLANC in the following sections.

4.2 Generative Process for Attributed Graph with GMM

In our method, we use a GMM as priors to guide the embedding learning and infer the nodes partitions for an attributed graph. The formulation of an attributed graph with $\mathbf{A}$ and $\mathbf{X}$ could be explained through a generative process as follows:

$$\begin{aligned}&p(\boldsymbol{c}; \boldsymbol{\pi}) = \mathrm{Cat}(\boldsymbol{\pi}) \\ &p(\boldsymbol{z}_i \mid \boldsymbol{c}_k = 1) = \mathcal{N}(\boldsymbol{\mu}_k, \mathbf{I}(\boldsymbol{\sigma}_k^2)) \\ &[\boldsymbol{\mu}_z, \boldsymbol{\sigma}_z] = f_{\boldsymbol{\theta}}(\mathbf{z}_i) \\ &p(\mathbf{A}_i \mid \boldsymbol{z}_i) = \begin{cases} \mathrm{Ber}\left(\boldsymbol{\mu}_z\right) & \text{if } \mathbf{A}_i \in \{0,1\}^N \\ \mathcal{N}\left(\boldsymbol{\mu}_z, \mathbf{I}\boldsymbol{\sigma}_z^2\right) & \text{if } \mathbf{A}_i \in \mathbb{R}^{\mathbb{N}} \end{cases}\end{aligned} \tag{3}$$

$$\begin{aligned}&p_{\boldsymbol{\theta}}(\boldsymbol{a}_j) = \mathcal{N}(0, \mathbf{I}) \\ &[\boldsymbol{\mu}_a, \boldsymbol{\sigma}_a] = f_{\boldsymbol{\theta}}(\mathbf{a}_j) \\ &p_{\boldsymbol{\theta}}(\mathbf{X}_{ij}|\boldsymbol{z}_i, \boldsymbol{a}_j) = \begin{cases} \mathrm{Ber}\left(\boldsymbol{\mu}_a^T \boldsymbol{\mu}_z\right) & \text{if } \mathbf{X}_{ij} \in \{0,1\} \\ \mathcal{N}\left(\boldsymbol{\mu}_a^T \boldsymbol{\mu}_z, \mathbf{I}\boldsymbol{\sigma}_a^2\right) & \text{if } \mathbf{X}_{ij} \in \mathbb{R} \end{cases}\end{aligned} \tag{4}$$

Eq. 3 shows the generative process network structure, where $\boldsymbol{z}_i \in \mathbf{Z}^{\mathcal{V}}$ and $\mathbf{A}_i$ are the embedding and neighborhood structure of the i^{th} node, respectively. The parameters for GMM priors are $\{\boldsymbol{\mu}, \boldsymbol{\sigma}, \boldsymbol{\pi}\}$. $f_{\boldsymbol{\theta}}(\cdot)$ is a neural network to learn the expectation of parameters. To generate the neighborhood structure for a node, we first need to sample an indicator vector $\boldsymbol{c} \in \{0,1\}^K$ from a categorical distribution $\mathrm{Cat}(\boldsymbol{\pi})$ to determine which Gaussian prior distribution would be used to generate the latent representation $\boldsymbol{z}_i$. Then, the network structure $\mathbf{A}_i$ could be generated from either multivariate Bernoulli or Gaussian distributions. The parameters $\boldsymbol{\mu}_x$ or $\boldsymbol{\sigma}_x$ are generated by a neural network $f_{\boldsymbol{\theta}}(\cdot)$. Similarly, Eq. 4 shows the generative process for attribute except that we assume that the latent representations of attributes follow a standard multivariate Gaussian distribution.

4.3 Evidence Lower Bound of VCLANC

Based on the generative process for an attribute graph, the joint probability distribution between the latent variables ($\boldsymbol{Z}^{\mathcal{V}}$, $\boldsymbol{Z}^{\mathcal{A}}$,

$\mathbf{C}$) and the observed variables $(\mathbf{A}, \mathbf{X})$ could be represented as follows:

$$\begin{aligned} &p_{\boldsymbol{\theta}}(\mathbf{A}, \mathbf{X}, \mathbf{Z}^{\mathcal{V}}, \mathbf{Z}^{\mathcal{A}}, \mathbf{C}) \\ &= p(\mathbf{C}) p(\mathbf{Z}^{\mathcal{V}} \mid \mathbf{C}) p(\mathbf{Z}^{\mathcal{A}}) p_{\boldsymbol{\theta}_1}(\mathbf{A} \mid \mathbf{Z}^{\mathcal{V}}) p_{\boldsymbol{\theta}_2}(\mathbf{X} \mid \mathbf{Z}^{\mathcal{A}}, \mathbf{Z}^{\mathcal{V}}). \end{aligned} \tag{5}$$

Then, according to Jensen's inequality, the *ELBO* of $\log p(\mathbf{A}, \mathbf{X})$ can be derived as follows:

$$\begin{aligned} &\log p(\mathbf{A}, \mathbf{X}) \\ &= \log \int_{\mathbf{Z}^{\mathcal{A}}} \int_{\mathbf{Z}^{\mathcal{V}}} \int_{\mathbf{C}} p_{\boldsymbol{\theta}}(\mathbf{A}, \mathbf{X}, \mathbf{Z}^{\mathcal{A}}, \mathbf{Z}^{\mathcal{V}}, \mathbf{C}) d_{\mathbf{Z}^{\mathcal{A}}} d_{\mathbf{Z}^{\mathcal{V}}} d_{\mathbf{C}} \\ &= \log \int_{\mathbf{Z}^{\mathcal{A}}} \int_{\mathbf{Z}^{\mathcal{V}}} \int_{\mathbf{C}} \frac{p_{\boldsymbol{\theta}}(\mathbf{A}, \mathbf{X}, \mathbf{Z}^{\mathcal{A}}, \mathbf{Z}^{\mathcal{V}}, \mathbf{C}) q_{\boldsymbol{\phi}}(\mathbf{Z}^{\mathcal{A}}, \mathbf{Z}^{\mathcal{V}}, \mathbf{C} \mid \mathbf{A}, \mathbf{X})}{q_{\boldsymbol{\phi}}(\mathbf{Z}^{\mathcal{A}}, \mathbf{Z}^{\mathcal{V}}, \mathbf{C} \mid \mathbf{A}, \mathbf{X})} \\ &d_{\mathbf{Z}^{\mathcal{A}}} d_{\mathbf{Z}^{\mathcal{V}}} d_{\mathbf{C}} \\ &\geq \mathbb{E}_{q_{\boldsymbol{\phi}}(\mathbf{Z}^{\mathcal{A}}, \mathbf{Z}^{\mathcal{V}}, \mathbf{C} \mid \mathbf{A}, \mathbf{X})} \left[\log \frac{p_{\boldsymbol{\theta}}(\mathbf{A}, \mathbf{X}, \mathbf{Z}^{\mathcal{A}}, \mathbf{Z}^{\mathcal{V}}, \mathbf{C})}{q_{\boldsymbol{\phi}}(\mathbf{Z}^{\mathcal{A}}, \mathbf{Z}^{\mathcal{V}}, \mathbf{C} \mid \mathbf{A}, \mathbf{X})} \right], \\ &\triangleq \mathcal{L}_e(\boldsymbol{\theta}, \boldsymbol{\phi}; \mathbf{A}, \mathbf{X}), \end{aligned} \tag{6}$$

where $\mathcal{L}_e(\boldsymbol{\theta}, \boldsymbol{\phi}; \mathbf{A}, \mathbf{X})$ is the ELBO for the marginal log-likelihood of the observed variables: $\mathbf{A}$ and $\mathbf{X}$. $q_{\boldsymbol{\phi}}(\mathbf{Z}^{\mathcal{A}}, \mathbf{Z}^{\mathcal{V}}, \mathbf{C} \mid \mathbf{A}, \mathbf{X})$ (abbreviated as $q_{\boldsymbol{\phi}}$ for simplicity) is a simpler distribution used to approximate the intractable true posterior $p(\mathbf{Z}^{\mathcal{A}}, \mathbf{Z}^{\mathcal{V}}, \mathbf{C} \mid \mathbf{A}, \mathbf{X})$. With the mean-field assumption, the latent variables are independent to each other and thus the posterior approximation $q_{\boldsymbol{\phi}}(\mathbf{Z}^{\mathcal{A}}, \mathbf{Z}^{\mathcal{V}}, \mathbf{C} \mid \mathbf{A}, \mathbf{X})$ could be factorized as follows:

$$\begin{aligned} &q_{\boldsymbol{\phi}}(\mathbf{Z}^{\mathcal{A}}, \mathbf{Z}^{\mathcal{V}}, \mathbf{C} \mid \mathbf{A}, \mathbf{X}) \\ &= q_{\boldsymbol{\phi}_1}(\mathbf{Z}^{\mathcal{A}} \mid \mathbf{X}) q_{\boldsymbol{\phi}_2}(\mathbf{Z}^{\mathcal{V}} \mid \mathbf{A}, \mathbf{X}) q_{\boldsymbol{\phi}_3}(\mathbf{C} \mid \mathbf{A}, \mathbf{X}) \end{aligned} \tag{7}$$

Therefore, the *ELBO* in Eq. 6 can be further decomposed by substituting Eq. 5 and 7 as follows:

$$\begin{aligned} &\mathcal{L}_e(\boldsymbol{\theta}, \boldsymbol{\phi}; \mathbf{A}, \mathbf{X}) \\ &= \mathbb{E}_{q_{\boldsymbol{\phi}}}[\log p_{\boldsymbol{\theta}_1}(\mathbf{A} \mid \mathbf{Z}^{\mathcal{V}})] \\ &+ \mathbb{E}_{q_{\boldsymbol{\phi}}}[\log p_{\boldsymbol{\theta}_2}(\mathbf{X} \mid \mathbf{Z}^{\mathcal{A}}, \mathbf{Z}^{\mathcal{V}})] \\ &- D_{KL}(q_{\boldsymbol{\phi}_1}(\mathbf{Z}^{\mathcal{A}} \mid \mathbf{X}) \parallel p(\mathbf{Z}^{\mathcal{A}})) \\ &- \sum_{\mathbf{C}} q_{\boldsymbol{\phi}_3}(\mathbf{C} \mid \mathbf{A}, \mathbf{X}) D_{KL}(q_{\boldsymbol{\phi}_2}(\mathbf{Z}^{\mathcal{V}} \mid \mathbf{A}, \mathbf{X}) \parallel p(\mathbf{Z}^{\mathcal{V}} \mid \mathbf{C})) \\ &- D_{KL}(q_{\boldsymbol{\phi}_3}(\mathbf{C} \mid \mathbf{A}, \mathbf{X}) \parallel p(\mathbf{C})). \end{aligned} \tag{8}$$

$q_{\boldsymbol{\phi}_1}(\mathbf{Z}^{\mathcal{A}} \mid \mathbf{X})$ and $q_{\boldsymbol{\phi}_2}(\mathbf{Z}^{\mathcal{V}} \mid \mathbf{A}, \mathbf{X})$ are the probabilistic encoders which produce the posterior approximation distributions (*e.g.*, Gaussian) given the input data $\mathbf{A}$ and $\mathbf{X}$. The encoders could have flexible structures for different tasks. As shown in Fig. 2, we use the graph convolutional network (GCN) for $q_{\boldsymbol{\phi}_2}(\mathbf{Z}^{\mathcal{V}} \mid \mathbf{A}, \mathbf{X})$ and the multilayer perceptron (MLP) for $q_{\boldsymbol{\phi}_1}(\mathbf{Z}^{\mathcal{A}} \mid \mathbf{X})$, respectively. Similarly, $p_{\boldsymbol{\theta}_1}(\mathbf{A} \mid \mathbf{Z}^{\mathcal{A}})$ and $p_{\boldsymbol{\theta}_2}(\mathbf{X} \mid \mathbf{Z}^{\mathcal{A}}, \mathbf{Z}^{\mathcal{V}})$ are the probabilistic decoders that given the latent representations, they would produce distribution for the observed data $\mathbf{A}$ and $\mathbf{X}$.

Following VAE [30], the priors and posterior approximations for the embeddings are set to be multivariate Gaussian distributions with diagonal covariance as follows:

$$\begin{aligned} &p(\mathbf{Z}_i^{\mathcal{V}} | c) \sim \mathcal{N}(\hat{\boldsymbol{\mu}}_c, \mathbf{I}\hat{\boldsymbol{\sigma}}_c^2) \\ &p(\mathbf{Z}^{\mathcal{A}}) = \mathcal{N}(0, \mathbf{I}\hat{\boldsymbol{\sigma}}_{\mathcal{A}}^2) \\ &q_{\boldsymbol{\phi}_1}(\mathbf{Z}_i^{\mathcal{A}} | \mathbf{X}) = \mathcal{N}(\boldsymbol{\mu}_{\mathcal{A}_i}, \mathbf{I}\boldsymbol{\sigma}_{\mathcal{A}_i}^2) \\ &q_{\boldsymbol{\phi}_2}(\mathbf{Z}_i^{\mathcal{V}} | \mathbf{A}, \mathbf{X}) = \mathcal{N}(\boldsymbol{\mu}_{\mathcal{V}_i}, \mathbf{I}\boldsymbol{\sigma}_{\mathcal{V}_i}^2). \end{aligned} \tag{9}$$

$\hat{\boldsymbol{\mu}}_c$ and $\hat{\boldsymbol{\sigma}}_c^2$ represent one of the Gaussian priors for node embedding distribution. We assume a normal Gaussian prior for attribute embeddings with mean and diagonal covariance as 0 and $\mathbf{I}\hat{\boldsymbol{\sigma}}_{\mathcal{A}}^2$, respectively. $\boldsymbol{\mu}_{\mathcal{V}_i}$,$\boldsymbol{\mu}_{\mathcal{A}_i}$,$\boldsymbol{\sigma}_{\mathcal{V}_i}^2$ and $\boldsymbol{\sigma}_{\mathcal{A}_i}^2$ are the parameters of Gaussian distributions for nodes and attributes embeddings determined by the encoders.

The KL divergence items in Eq. 8 have analytical form. As for the first two expectation terms in Eq.8, we could apply the reparameterization trick and stochastic gradient variational Bayes (SGVB) [30] to compute the expectations with the Monte Carlo estimation. Hence, the ELBO of Eq. 8 could be written as:

$$\begin{aligned} &\mathcal{L}_e(\boldsymbol{\theta}, \boldsymbol{\phi}; \mathbf{A}, \mathbf{X}) \\ &= \frac{1}{LN^2} \sum_{l=1}^{L} \sum_{i,j \in \mathcal{V}} \left[\log p_{\boldsymbol{\theta}_1}(\mathbf{A}_{ij} \mid \mathbf{Z}_i^{\mathcal{V}(l)}, \mathbf{Z}_j^{\mathcal{V}(l)}) \right] \\ &+ \frac{1}{LMN} \sum_{l=1}^{L} \sum_{i \in \mathcal{A}, j \in \mathcal{V}} \left[\log p_{\boldsymbol{\theta}_2}(\mathbf{X}_{ij} \mid \mathbf{Z}_i^{\mathcal{A}(l)}, \mathbf{Z}_j^{\mathcal{V}(l)}) \right] \\ &- \frac{1}{2MJ} \sum_{i=1}^{M} \sum_{j=1}^{J} \left[\frac{\boldsymbol{\sigma}_{\mathcal{A}_i}^2|_j}{\hat{\boldsymbol{\sigma}}_{\mathcal{A}_i}^2|_j} + \frac{\boldsymbol{\mu}_{\mathcal{A}_i}^2|_j}{\hat{\boldsymbol{\sigma}}_{\mathcal{A}_i}^2|_j} - \log \frac{\boldsymbol{\sigma}_{\mathcal{A}_i}^2|_j}{\hat{\boldsymbol{\sigma}}_{\mathcal{A}_i}^2|_j} - 1 \right] \\ &- \frac{1}{2NKJ} \sum_{i=1}^{N} \sum_{c=1}^{K} \gamma_{i,c} \sum_{j=1}^{J} \left[\frac{\boldsymbol{\sigma}_{\mathcal{V}_i}^2|_j}{\hat{\boldsymbol{\sigma}}_c^2|_j} + \frac{(\boldsymbol{\mu}_{\mathcal{V}_i}|_j - \hat{\boldsymbol{\mu}}_c|_j)^2}{\boldsymbol{\sigma}_c^2|_j} \right. \\ &\left. - \log \frac{\boldsymbol{\sigma}_{\mathcal{V}_i}^2|_j}{\hat{\boldsymbol{\sigma}}_c^2|_j} - 1 \right] - \frac{1}{NK} \sum_{i=1}^{N} \sum_{c=1}^{K} \gamma_{i,c} \log \frac{\gamma_{i,c}}{\pi_c}, \end{aligned} \tag{10}$$

where

$$\begin{aligned} \mathbf{Z}_i^{\mathcal{V}(l)} &= \boldsymbol{\mu}_{\mathcal{V}_i} + \boldsymbol{\sigma}_{\mathcal{V}_i} \odot \boldsymbol{\epsilon}^{(l)}, \text{ with } \boldsymbol{\epsilon}^{(l)} \sim \mathcal{N}(0, \mathbf{I}) \\ \mathbf{Z}_j^{\mathcal{V}(l)} &= \boldsymbol{\mu}_{\mathcal{V}_j} + \boldsymbol{\sigma}_{\mathcal{V}_j} \odot \boldsymbol{\epsilon}^{(l)}, \text{ with } \boldsymbol{\epsilon}^{(l)} \sim \mathcal{N}(0, \mathbf{I}) \\ \mathbf{Z}_i^{\mathcal{A}(l)} &= \boldsymbol{\mu}_{\mathcal{A}_i} + \boldsymbol{\sigma}_{\mathcal{A}_i} \odot \boldsymbol{\epsilon}^{(l)}, \text{ with } \boldsymbol{\epsilon}^{(l)} \sim \mathcal{N}(0, \mathbf{I}). \end{aligned}$$

In Eq. 10, L represents the size of Monte Carlo sampling to estimate the expectations and $\cdot|_j$ denotes the j^{th} element of the vector. $\gamma_{i,c}$ represents $q_{\boldsymbol{\phi}_3}(\mathbf{C}_{i,c} | \mathbf{A}_i, \mathbf{X}_i)$ for simplicity. $\odot$ denotes the element-wise product between the auxiliary noise from $\mathcal{N}(0, \mathbf{I})$ and the posterior distribution. To optimize Eq. 10, we need to choose detailed inference network $f_{\boldsymbol{\phi}}$ and generative network $g_{\boldsymbol{\theta}}$ as encoders and decoders to simulate $q_{\boldsymbol{\phi}}$ and $p_{\boldsymbol{\theta}}$, respectively.

Inference network $f_{\boldsymbol{\phi}}$. As shown in Fig. 2, the inference network $f_{\boldsymbol{\phi}}$ is parameterized by a two-layer GCN and a two-layer multilayer perceptron (MLP) for inferring the means and variances of $q_{\boldsymbol{\phi}_1}(\mathbf{Z}^{\mathcal{A}} \mid \mathbf{X})$ and $q_{\boldsymbol{\phi}_2}(\mathbf{Z}^{\mathcal{V}} \mid \mathbf{A}, \mathbf{X})$, respectively. Specifically, the two-layer GCN inference network is organized as:

$$\begin{aligned} \mathbf{H}_{\mathcal{V}}^{(1)} &= \mathrm{ReLU}\left(\tilde{\mathbf{A}}\mathbf{X}\mathbf{W}_{\mathcal{V}}^{(0)}\right) \\ \left[\boldsymbol{\mu}_{\mathcal{V}}, \boldsymbol{\sigma}_{\mathcal{V}}^2\right] &= \tilde{\mathbf{A}}\mathbf{H}_{\mathcal{V}}^{(1)}\mathbf{W}_{\mathcal{V}}^{(1)}, \end{aligned} \tag{11}$$

where $\left[\boldsymbol{\mu}_{\mathcal{V}}, \boldsymbol{\sigma}_{\mathcal{V}}^2\right]$ are the learned parameters for the posterior approximation distribution $q_{\boldsymbol{\phi}_2}(\mathbf{Z}^{\mathcal{V}} | \mathbf{A}, \mathbf{X})$. $\mathrm{ReLU}(\cdot) = max(0, \cdot)$ is rectified linear unit, a popular activation function. $\boldsymbol{\phi}_2 = [\mathbf{W}_{\mathcal{V}}^{(0)}, \mathbf{W}_{\mathcal{V}}^{(1)}]$ are the trainable weight matrices for the two-layer GCN. $\tilde{\mathbf{A}} = \mathbf{D}^{-\frac{1}{2}}\mathbf{A}\mathbf{D}^{-\frac{1}{2}}$ is the symmetrically normalized adjacency matrix of $\mathcal{G}$ with $\mathbf{D}_{ii} = \sum_j \mathbf{A}_{ij}$ being the degree matrix.

The two-layer MLP is defined as:

$$\begin{aligned} \mathbf{H}_{\mathcal{A}}^{(1)} &= \tanh\left(\mathbf{X}^T\mathbf{W}_{\mathcal{A}}^{(0)} + \mathbf{b}^{(0)}\right) \\ \left[\boldsymbol{\mu}_{\mathcal{A}}, \boldsymbol{\sigma}_{\mathcal{A}}^2\right] &= \mathbf{H}_{\mathcal{A}}^{(1)}\mathbf{W}_{\mathcal{A}}^{(1)} + \mathbf{b}^{(1)}, \end{aligned} \tag{12}$$

where $\left[\boldsymbol{\mu}_{\mathcal{A}}, \boldsymbol{\sigma}_{\mathcal{A}}^2\right]$ are the parameters for the posterior approximation distribution $q_{\boldsymbol{\phi}_1}(\mathbf{Z}_i^{\mathcal{A}} | \mathbf{X})$. $\tanh(\cdot)$ denotes the tangent activation function. $\boldsymbol{\phi}_1 = [\mathbf{W}_{\mathcal{A}}^{(0)}, \mathbf{W}_{\mathcal{A}}^{(1)}, \mathbf{b}^{(0)}, \mathbf{b}^{(1)}]$ are the

trainable weights in the two- layer MLP encoder. Based on the Gaussian embeddings learned by the inference networks, the reparameterization trick [18], [30] will be used to reparameterize the latent embeddings for nodes and attributes in a differentiable way to jointly optimize the inference network and generative network.

Generative network $g_{\boldsymbol{\theta}}$. The generative network is used to simulate $p_{\boldsymbol{\theta}_1}(\mathbf{A} \mid \mathbf{Z}^{\mathcal{V}})$ (*abbr.* $p_{\boldsymbol{\theta}_1}$) and $p_{\boldsymbol{\theta}_2}(\mathbf{X} \mid \mathbf{Z}^{\mathcal{A}}, \mathbf{Z}^{\mathcal{V}})$ (*abbr.* $p_{\boldsymbol{\theta}_2}$) to maximize the likelihood of the observed variable $\mathbf{A}$ and $\mathbf{X}$. Since both the adjacent matrix $\mathbf{A}$ and the feature matrix $\mathbf{X}$ of the graph $\mathcal{G}$ are binary-valued in our experimental datasets, we set the generative network to learn the best parameters of Bernoulli distributions for the observed nodes and attributes as:

$$
\begin{aligned}
&p_{\boldsymbol{\theta}_1}\left(\mathbf{A}_{ij} \mid \mathbf{Z}_i^{\mathcal{V}}, \mathbf{Z}_j^{\mathcal{V}}\right) = \mathrm{Ber}\left(\tilde{\boldsymbol{\mu}}_{\mathcal{V}_{ij}}\right),\ \tilde{\boldsymbol{\mu}}_{\mathcal{V}_{ij}} = g_{\boldsymbol{\theta}_1}(\mathbf{Z}_i^{\mathcal{V}}, \mathbf{Z}_j^{\mathcal{V}}) \\
&p_{\boldsymbol{\theta}_2}\left(\mathbf{X}_{ij} \mid \mathbf{Z}_i^{\mathcal{V}}, \mathbf{Z}_j^{\mathcal{A}}\right) = \mathrm{Ber}\left(\tilde{\boldsymbol{\mu}}_{\mathcal{A}_{ij}}\right),\ \tilde{\boldsymbol{\mu}}_{\mathcal{A}_{ij}} = g_{\boldsymbol{\theta}_2}(\mathbf{Z}_i^{\mathcal{V}}, \mathbf{Z}_j^{\mathcal{A}}),
\end{aligned}
$$

where

$$
\begin{aligned}
&g_{\boldsymbol{\theta}_1}(\mathbf{Z}_i^{\mathcal{V}}, \mathbf{Z}_j^{\mathcal{V}}) = \mathrm{sigmoid}(\mathbf{Z}_i^{\mathcal{V}T}\mathbf{Z}_j^{\mathcal{V}}) \\
&g_{\boldsymbol{\theta}_2}(\mathbf{Z}_i^{\mathcal{V}}, \mathbf{Z}_j^{\mathcal{A}}) = \mathrm{sigmoid}(\mathbf{Z}_i^{\mathcal{V}T}\mathbf{Z}_j^{\mathcal{A}}).
\end{aligned} \tag{13}
$$

The encoder $g_{\boldsymbol{\theta}_1}(\cdot)$ and $g_{\boldsymbol{\theta}_2}(\cdot)$ use simple inner product between latent variables with sigmoid activation function. Hence, the log likelihood of $p_{\boldsymbol{\theta}_1}\left(\mathbf{A}_{ij} \mid \mathbf{Z}_i^{\mathcal{V}}, \mathbf{Z}_j^{\mathcal{V}}\right)$ and $p_{\boldsymbol{\theta}_2}\left(\mathbf{X}_{ij} \mid \mathbf{Z}_i^{\mathcal{V}}, \mathbf{Z}_j^{\mathcal{A}}\right)$ can be computed as follows:

$$
\begin{aligned}
p_{\boldsymbol{\theta}_1} &= \sum_{d=1}^{J} \mathbf{A}_{ij} \log(\tilde{\boldsymbol{u}}_{\mathcal{V}_{ij}}) + (1 - \mathbf{X}_{ij})(1 - \tilde{\boldsymbol{u}}_{\mathcal{V}_{ij}}) \\
p_{\boldsymbol{\theta}_2} &= \sum_{d=1}^{J} \mathbf{X}_{ij} \log(\tilde{\boldsymbol{u}}_{\mathcal{A}_{ij}}) + (1 - \mathbf{X}_{ij})(1 - \tilde{\boldsymbol{u}}_{\mathcal{A}_{ij}})
\end{aligned} \tag{14}
$$

For the real-value weighted datasets, we could replace the Bernoulli distribution with Gaussian distribution.

4.4 Node Clustering Inference

The latent variable $\mathbf{C}$ that represents the chosen Gaussian priors for latent node embeddings is used for node clustering assignments. To infer $\mathbf{C}$, we need to derive the analytical form for $q_{\boldsymbol{\phi}_3}(\mathbf{C} \mid \mathbf{A}, \mathbf{X})$. However, directly inferring $\mathbf{C}$ is nontrivial since it is difficult to find an appropriate distribution for $q_{\boldsymbol{\phi}_3}(\mathbf{C} \mid \mathbf{A}, \mathbf{X})$. Therefore, similar to VaDE [32], we resort to find an approximation distribution for $q_{\boldsymbol{\phi}_3}(\mathbf{C} \mid \mathbf{A}, \mathbf{X})$.

The evidence lower bound of $\log p(\mathbf{A}, \mathbf{X})$ in Eq. 6 could be rewritten as:

$$
\begin{aligned}
&\mathcal{L}_e(\boldsymbol{\theta}, \boldsymbol{\phi}; \mathbf{A}, \mathbf{X}) \\
&= \mathbb{E}_{q_{\boldsymbol{\phi}}}\left[\log \frac{p(\mathbf{A}, \mathbf{X} \mid \mathbf{Z}^{\mathcal{A}}, \mathbf{Z}^{\mathcal{V}}, \mathbf{C}) p(\mathbf{Z}^{\mathcal{A}}, \mathbf{Z}^{\mathcal{V}}, \mathbf{C})}{q_{\boldsymbol{\phi}}(\mathbf{Z}^{\mathcal{A}}, \mathbf{Z}^{\mathcal{V}}, \mathbf{C} \mid \mathbf{A}, \mathbf{X})}\right] \\
&= \mathbb{E}_{q_{\boldsymbol{\phi}}}\left[\log \frac{p(\mathbf{A}, \mathbf{X} \mid \mathbf{Z}^{\mathcal{A}}, \mathbf{Z}^{\mathcal{V}}, \mathbf{C}) p(\mathbf{Z}^{\mathcal{A}}) p(\mathbf{Z}^{\mathcal{V}}) p(\mathbf{C} \mid \mathbf{Z}^{\mathcal{V}})}{q_{\boldsymbol{\phi}}(\mathbf{Z}^{\mathcal{A}}, \mathbf{Z}^{\mathcal{V}}, \mathbf{C} \mid \mathbf{A}, \mathbf{X})}\right] \\
&= \mathbb{E}_{q_{\boldsymbol{\phi}}}\left[\log \frac{p(\mathbf{A}, \mathbf{X} \mid \mathbf{Z}^{\mathcal{A}}, \mathbf{Z}^{\mathcal{V}}, \mathbf{C}) p(\mathbf{Z}^{\mathcal{A}}) p(\mathbf{Z}^{\mathcal{V}})}{q_{\boldsymbol{\phi}}(\mathbf{Z}^{\mathcal{A}}, \mathbf{Z}^{\mathcal{V}} \mid \mathbf{A}, \mathbf{X})}\right] \\
&- \mathbb{E}_{q_{\boldsymbol{\phi}}}\Big[D_{KL}(q_{\boldsymbol{\phi}_3}(\mathbf{C} \mid \mathbf{A}, \mathbf{X}) \parallel p(\mathbf{C} \mid \mathbf{Z}^{\mathcal{V}})\Big]
\end{aligned} \tag{15}
$$

In Eq. 15, the expectation of KL divergence *w.r.t.* $q_{\boldsymbol{\phi}}$ is non-negative and it becomes zero only if the two distributions in D_{KL} are identical. Therefore, the *ELBO* of $\log p(\mathbf{A}, \mathbf{X})$ could become even tighter if $q_{\boldsymbol{\phi}_3}(\mathbf{C} \parallel \mathbf{A}, \mathbf{X}) = p(\mathbf{C} \mid \mathbf{Z}^{\mathcal{V}})$. We assume $q_{\boldsymbol{\phi}_3}(\mathbf{C} \mid \mathbf{A}, \mathbf{X}) = \prod_{i=1}^{N} q_{\boldsymbol{\phi}_3}(\mathbf{C}_i \mid \mathbf{A}_i, \mathbf{X}_i)$ and $p(\mathbf{C} \mid \mathbf{Z}^{\mathcal{V}}) = \prod_{i=1}^{N} p(\mathbf{C}_i \mid \mathbf{Z}_i^{\mathcal{V}})$. Thus, we set $q_{\boldsymbol{\phi}_3}(\mathbf{C}_i \mid \mathbf{A}_i, \mathbf{X}_i) = p(\mathbf{C}_i \mid \mathbf{Z}_i^{\mathcal{V}})$ and get $q_{\boldsymbol{\phi}_3}(\mathbf{C} \mid \mathbf{A}, \mathbf{X}) = p(\mathbf{C} \mid \mathbf{Z}^{\mathcal{V}})$. According to the Bayes' rule, the probability for $p(\mathbf{C}_i \mid \mathbf{Z}_i^{\mathcal{V}})$ could be computed as:

$$
p(\mathbf{C}_i \mid \mathbf{Z}_i^{\mathcal{V}}) = \frac{p(\mathbf{Z}_i^{\mathcal{V}} \mid \mathbf{C}_i) p(\mathbf{C}_i)}{\sum\limits_{\mathbf{C}} p(\mathbf{Z}_i^{\mathcal{V}} \mid \mathbf{C}) p(\mathbf{C})}, \tag{16}
$$

where $p(\mathbf{Z}_i^{\mathcal{V}} \mid \mathbf{C}_i) p(\mathbf{C}_i)$ is based on the generative process for nodes with Gaussian mixture model as priors. It is worth noting that the calculation for $p(\mathbf{C}_i \mid \mathbf{Z}_i^{\mathcal{V}})$ is in the embeddings space rather than the raw features of the nodes. Hence, it becomes clear that the clustering assignments of nodes could be inferred simultaneously with the variational co-embedding learning process.

4.5 Clustering Assignment Hardening

In order to further strengthen the clustering performance using the Gaussian mixture priors, we exploit a clustering assignment hardening loss from DEC [33] to put more emphasis on the highly confident node clustering assignment.

First, we compute a soft assignment distribution $\mathbf{Q}$ for each node against different Gaussian prior centers using Eq. 17. The node probability distribution against each Gaussian prior is measured by Student's t-distribution. α is the degree of freedom and is set as one in our experiments.

$$
\mathbf{Q}_{ic} = \frac{\left(1 + \left\|\mathbf{Z}_i^{\mathcal{V}} - \boldsymbol{\mu}_c\right\|^2 / \alpha\right)^{-\frac{\alpha+1}{2}}}{\sum_{c'} \left(1 + \left\|\mathbf{Z}_i^{\mathcal{V}} - \boldsymbol{\mu}_{c'}\right\|^2 / \alpha\right)^{-\frac{\alpha+1}{2}}} \tag{17}
$$

$$
\mathbf{P}_{ic} = \frac{\mathbf{Q}_{ic}^2 / \Sigma_i \mathbf{Q}_{ic}}{\sum_{c'} \mathbf{Q}_{ic'}{}^2 / \Sigma_i \mathbf{Q}_{ic'}} \tag{18}
$$

Then, the soft assignment distribution $\mathbf{Q}$ is further squared and normalized to have stricter probabilities with Eq. 18. Finally, the KL divergence is adopted to between $\mathbf{P}$ and $\mathbf{Q}$ using Eq. 19 to push $\mathbf{Q}$ put more emphasis on the highly confident soft assignment by optimizing the neural network parameters and the trainable Gaussian mixture priors.

$$
\mathcal{L}_h = \mathrm{KL}(\mathbf{P} \| \mathbf{Q}) = \sum_i \sum_c \mathbf{P}_{ic} \log \frac{\mathbf{P}_{ic}}{\mathbf{Q}_{ic}} \tag{19}
$$

4.6 Mutual Distance for Gaussian Priors

To avoid the Gaussian mixture priors collapsing to each other during the training process, we further design a mutual distance loss to force the Gaussian centers of different priors to move away from each other. As a result, the regularized latent node embedding distributions by Gaussian mixture priors could become more distinguishable for different node categories.

$$
\mathcal{L}_m = \frac{1}{K^2} \sum_{c=1}^{K} \sum_{k=1}^{K} \|\boldsymbol{\mu}_c - \boldsymbol{\mu}_k\|_2 \tag{20}
$$

The mutual distance between Gaussian priors is defined in Eq. 20, which averaging the Euclidean distance among all the Gaussian centers. During the training process, the mutual distance loss is maximized through updating the trainable means of different Gaussian priors.

Algorithm 1: VCLANC

Input: attributed graph $\mathcal{G}$; embedding size J; hyper-parameters ω and β; training epochs T_1 and T_2; Gaussian parameter updating interval T.
Output: node embedding $\mathbf{Z}^{\mathcal{V}}$; node clustering assignments.

1 **for** $epoch \leftarrow 1$ **to** T_1 **do**
2 | update $\{\phi, \boldsymbol{\theta}\}$.
3 **end**
4 Apply GMM on $\mathbf{Z}^{\mathcal{V}}$ to get $\{\boldsymbol{\mu}, \boldsymbol{\sigma}, \boldsymbol{\pi}\}$.
5 **for** $epoch \leftarrow 1$ **to** T_2 **do**
6 | **if** $epoch\%10 < T$ **then**
7 | | update $\{\phi, \boldsymbol{\theta}\}$.
8 | **end**
9 | **else**
10 | | update $\{\boldsymbol{\mu}, \boldsymbol{\sigma}, \boldsymbol{\pi}\}$.
11 | **end**
12 **end**
13 Compute clustering assignment using Eq. 16.

4.7 Model Training

Our final objective function unifies the *ELBO* $\mathcal{L}_e$, the cluster assignment hardening loss $\mathcal{L}_h$ and the mutual distance loss $\mathcal{L}_m$ to jointly optimize the parameters of the proposed model.

$$\mathcal{L} = \mathcal{L}_e + \beta\mathcal{L}_m - \omega\mathcal{L}_h \tag{21}$$

As shown in Eq. 21, ω and β are the weight coefficients to adjust the contributions of the cluster assignment hardening loss (Eq. 19) and the mutual distance loss (Eq. 20). We optimize Eq. 21 with gradient descent based optimizer to update the model parameters *w.r.t.* $\{\phi, \boldsymbol{\theta}, \boldsymbol{\mu}, \boldsymbol{\sigma}, \boldsymbol{\pi}\}$. ϕ and $\boldsymbol{\theta}$ are the trainable weights for the inference and generative networks. $\{\boldsymbol{\mu}, \boldsymbol{\sigma}, \boldsymbol{\pi}\}$ are the trainable parameters of the Gaussian mixture priors.

We first train the inference and generative network for node embeddings without updating the Gaussian parameters. Then, an external GMM cluster model is applied on the node embeddings to initialize the parameters of the internal Gaussian priors in VCLANC. Finally, we optimize the network parameters and the Gaussian parameters intermittently. The final clustering assignment for each node could be derived based on Eq. 16. Algorithm 1 summarizes our proposed method. From line 1 to line 3, the algorithm only updates the parameters $\{\phi, \boldsymbol{\theta}\}$ for the inference and generative network to get initial node embeddings. Then, the internal Gaussian prior parameters $\{\boldsymbol{\mu}, \boldsymbol{\sigma}, \boldsymbol{\pi}\}$ are initialized by GMM from the current node embedding space in line 4. After that, the algorithm performs iterative updating for the neural networks and the Gaussian mixture priors to form better clusters. Finally, the node embeddings $\mathbf{Z}^{\mathcal{V}}$ and the clustering assignments could be easily derived based on the trained network and the Gaussian mixture priors.

5 Experimental Setup

In this section, we introduce our experimental setup including the compared baselines and parameter settings, the adopted datasets and evaluation metrics.

5.1 Baselines and Parameter Settings

We introduce all the adopted baselines and their parameter settings as follows:

- K-means [34] is a partition based clustering algorithm to iteratively divide the data into K number of groups and update the cluster centers until the cluster centers become stable.
- Gaussian mixture model (GMM) is a probabilistic clustering model which assumes the data are generated from a Gaussian mixture distributions and the cluster indexes for the data are determined by the component assignment probability.
- GAE [18] is an unsupervised embedding learning method for graph-structured data based on the auto-encoder framework. GAE adopts GCN as encoder and an inner product as decoder.
- VGAE [18] is a probabilistic variant of GAE. Compared with GAE, VGAE assumes a prior distribution on the latent node embeddings and optimizes the model through minimizing the KL divergence regularized reconstruction loss between inputs and outputs.
- CAN [35] is an extension of VGAE. The difference between VGAE and CAN is that CAN jointly learns the embeddings for nodes and attributes using an extra auto-encoder network to process the node attributes.
- SDCN [6] uses a delivery operator to transfer the knowledge learned by a deep autoencoder to the corresponding deep GCN. Then, a dual self-supervised mechanism is used to unify these two modules and guide the update of the whole network.
- NEC [5] is an extension of GAE to detect the attributed network communities using a soft clustering assignment loss and a network modularity loss.

The parameter settings for all the methods are detailed as follows. The main parameter for K-means and GMM is the number of clusters, which is set as the actual cluster size of the datasets. The other parameters of K-means and GMM are set as default following scikit-learn package [1]. We adopt the same parameter settings for GAE, VGAE, CAN, NEC and VCLANC on all the datasets. Specifically, the total training epoch is set as 300 and Adam optimizer [36] is adopted with the learning rate as 0.002. The two-layer GCN is set with the hidden dimension as 64 and 32, respectively. For SDCN, we follow their parameter settings with the dimension of the latent layers set as 500-500-2000-10, the learning rate set as 0.0001 and epochs set as 50 [6]. For the proposed method, we first train the model for 200 epochs only using the ELBO $\mathcal{L}_e$. Then, we use GMM to initialize the parameters for the Gaussian mixture priors. After that, we train the model with the complete objective function in Eq. 21 and update the Gaussian parameters intermittently with $T = 5$ in the remaining 100 epochs (shown in Algorithm 1). The two hyper-parameters ω and β are set as one. We use the machine learning library Pytorch [2] to implement the neural network related methods.

5.2 Datasets

We conduct experiments on four attributed network datasets with the cluster size of nodes no less than six. The statistics

1. https://scikit-learn.org/stable/index.html
2. https://pytorch.org/

Table 2
Statistics of the datasets.

Dataset	#Nodes	#Edges	#Attributes	#Clusters
Cora	2,708	5,429	1,433	7
Citeseer	3,327	4,732	3,703	6
BlogCatalog	5,196	171,743	8,189	6
Flickr	7,575	239,738	12,047	9

of the datasets are shown in Table 2. The *Cora* and Citeseer datasets are created from citation networks by Sen *et al.* [37]. The nodes represents articles and the edges are their citation actions. Attributes of each node are a list keywords. The *BlogCatalog* [38] and *Flickr* [39] datasets are created from social networks. The edges represent the users' relationships and the attributes are the keywords extracted from the users' profiles. The ground-truth cluster information of nodes in each dataset is included and could be used to evaluate the clustering performance of the different methods.

5.3 Evaluation Metrics

We use six metrics to evaluate the clustering performance. Suppose that the predicted partition and the true partition of a network are represented as $\Omega = \{\omega_1, \cdots, \omega_q\}$ and $\mathcal{C} = \{c_1, \cdots, c_p\}$, respectively. Larger score implies better clustering performance across all the metrics. Each of the metrics are briefly introduced in the follow.

- **NMI** is metric used to determine the clustering quality by computing normalized mutual information between the predicted partitions and the true partitions. Its definition is shown as follows:

$$\mathrm{NMI}(\Omega, \mathcal{C}) = \frac{\sum_{i,j} \frac{|w_i \cap c_j|}{N} \log \frac{N|w_i \cap c_j|}{|w_i||c_j|}}{(-\sum_i \frac{|w_j|}{N} \log \frac{|w_i|}{N} - \sum_j \frac{|c_j|}{N} \log \frac{|c_j|}{N})/2}. \tag{22}$$

- **Purity**. Ideally, the predicted partition should contain only the data objects from one categories. This metric is used to evaluate the average pure level among all the predicted partitions. It is defined as follows:

$$\mathrm{Purity}\ (\Omega, \mathcal{C}) = \frac{1}{N} \sum_{i=1}^{k} \max_j |c_i \cap \omega_j|\,. \tag{23}$$

- **ARI** is an adjust version of Rand Index which is used to calculate the percentage of the correct clustering assignments. ARI is defined as follows:

$$ARI(\Omega, \mathcal{C}) = \frac{\sum_{i,j} \binom{|\omega_i \cap c_j|}{2} - [\sum_i \binom{|\omega_i|}{2} \sum_j \binom{|c_j|}{2}]/\binom{n}{2}}{\frac{1}{2}[\sum_i \binom{|\omega_i|}{2} + \sum_j \binom{|c_j|}{2}] - [\sum_i \binom{|\omega_i|}{2} \sum_j \binom{|c_j|}{2}]/\binom{n}{2}}, \tag{24}$$

- **Precision (P)** denotes the percentage of predicted results which are truly relevant for a class. For a dataset with multiple classes, we use weighted precision score to avoid the imbalanced issue. Let TP_i denotes the true positive prediction number, FP_i denotes the false positive prediction number, and FN_i denotes the false negative prediction number for the i^{th} class, respectively. The weighted precision is defined as:

$$\text{Precision} = \sum_i \frac{|c_i|}{N} \frac{TP_i}{TP_i + FP_i}.$$

- **Recall (R)** denotes the rate of relevant results that were truly identified for a class. For multi-class dataset, we use the weighted recall defined as:

$$\text{Recall} = \sum_i \frac{|c_i|}{N} \frac{TP_i}{TP_i + FN_i}.$$

- **F1-score (F1)** is the harmonic mean of precision and recall for a class. For multi-class dataset, the weighted F1-score is defined as:

$$\text{F1-score} = \sum_i \frac{|c_i|}{N} \frac{2TP_i}{2TP_i + FP_i + FN_i}.$$

6 Results and Analysis

In this section, we report the experimental results for all the compared methods.

6.1 Clustering Performance

Tables 3, 4, 5 and 6 show the clustering performance of all the methods on the adopted datasets. We repeat the experiment on each dataset for 10 times to report the average performance. The best and second best results are marked with *boldface* and *underline*, respectively.

As we can see from Table 3 to Table 6, the proposed VCLANC consistently achieves the best or second best clustering performance over its baselines on the adopted datasets. Let us first look through the results from the first group of baselines, which include K-means and GMM methods. These two general clustering methods show quite poor performance across all the datasets. For example, the NMI value of K-Means and GMM on Cora dataset is 0.143 and 0.0772, which is far behind VCLANC with its NMI as 0.5334. Similarly, the F1-score of K-means and GMM is 0.3318 and 0.2226, which is also worse compared with VCLANC with F1-score as 0.7004 and CAN with its F1-score as 0.6769. Interestingly, the precision of K-means and GMM achieve surprised high score on Flickr dataset in Table 6. However, this do not denote that K-means and GMM are better than the other methods on Flickr dataset as their recall value is quite low. K-means and GMM can only perform black-box style clustering on the input data and they are not flexible to fuse different types of information such as the network structure and the node attribute. But it has been proved that fusing both the network structure and the node attributes is useful for the attributed network clustering task.

The second group of baselines in our experiments include GAE, VGAE and CAN, which first learn node embeddings and then use K-means for the clustering task. As shown in Tables from 3 to 6, the overall clustering performance of GAE, VGAE and CAN is better than directly using K-means or GMM. The performance improvements show that learning low-dimensional representation for the network is quite important in network clustering. For instance, the NMI value of GAE and VGAE is around 0.46 on Cora dataset which is much better than K-means and GMM. Similarly, the F1-score of GAE and VGAE is around 0.64 on Cora dataset which is also far better than K-means or GMM. Among GAE, VGAE and CAN, we can see that the performance of GAE is slightly worse

Table 3
Clustering performance on Cora dataset.

	NMI	Purity	ARI	F1	P	R
K-means	0.1430	0.3811	0.0734	0.3318	0.4257	0.3242
GMM	0.0772	0.3310	0.0294	0.2266	0.4026	0.3133
GAE	0.4597	0.6526	0.3538	0.6291	0.7272	0.6058
VGAE	0.461	0.6536	0.3693	0.6433	0.72	0.6175
CAN	0.4893	0.6842	0.4361	0.6769	0.7286	0.6579
SDCN	0.2199	0.4944	0.1658	0.4397	0.5103	0.4111
NEC	0.4481	0.6224	0.3799	0.5865	0.6418	0.5694
VCLANC	**0.5334**	**0.7085**	**0.4841**	**0.7004**	**0.7504**	**0.6816**

Table 4
Clustering performance on Citeseer dataset.

	NMI	Purity	ARI	F1	P	R
K-means	0.2215	0.4724	0.1758	0.4625	0.5243	0.4519
GMM	0.1756	0.4036	0.1287	0.3444	0.4687	0.3949
GAE	0.1885	0.4235	0.0799	0.3834	0.5579	0.3808
VGAE	0.2426	0.5053	0.1554	0.4706	0.58	0.4618
CAN	0.3651	0.6464	0.3384	0.5976	0.6381	0.5950
SDCN	0.3842	0.6631	0.4022	0.6460	0.6454	0.6567
NEC	0.319	0.5882	0.2867	0.5352	0.5772	0.5307
VCLANC	**0.4007**	**0.6769**	**0.4070**	**0.6560**	**0.6791**	**0.6439**

Table 5
Clustering performance on BlogCatalog dataset.

	NMI	Purity	ARI	F1	P	R
K-means	0.1659	0.3249	0.0679	0.2632	0.4481	0.3079
GMM	0.1733	0.3096	0.0602	0.2194	0.459	0.3042
GAE	0.1389	0.3449	0.0866	0.3009	0.3191	0.3104
VGAE	0.2609	0.4622	0.1721	0.4278	0.4846	0.4289
CAN	0.2919	0.505	0.1996	0.4556	0.5101	0.4600
SDCN	0.2743	0.4390	0.1947	0.3755	0.3790	0.4024
NEC	0.2735	0.4929	0.1977	0.4347	0.4533	0.4355
VCLANC	**0.3036**	**0.5254**	**0.2455**	**0.4884**	**0.5146**	**0.4935**

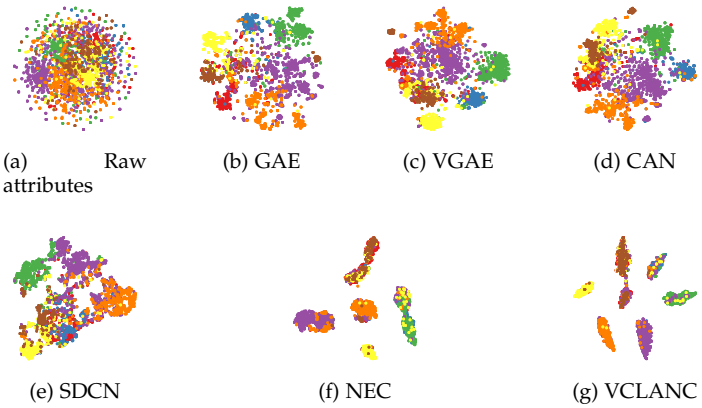
Table 6
Clustering performance on Flickr dataset.

	NMI	Purity	ARI	F1	P	R
K-means	0.0552	0.1313	0.0006	0.0484	0.4459	0.1294
GMM	0.048	0.1282	0.0003	0.0444	**0.4617**	0.1267
GAE	0.1521	0.2828	0.0783	0.2322	0.2693	0.2529
VGAE	0.1116	0.2485	0.0601	0.2034	0.2092	0.2290
CAN	0.1763	0.3083	0.0990	0.2736	0.3018	0.2936
SDCN	**0.2682**	**0.3154**	**0.1665**	0.2488	0.3163	**0.3125**
NEC	0.1299	0.2657	0.0744	0.2347	0.2366	0.2362
VCLANC	0.1850	0.3127	0.1216	**0.2943**	0.3343	0.3086

than VGAE and CAN. CAN achieves better performance than VGAE and also ranks as the second best among all the methods on the Cora, Citeseer and BlogCatalog. Compared with VGAE, CAN adds extra module to embed the attributes of the network into the same semantic space to learn the affinities between attributes and network structures. The experimental results of CAN prove that its co-embedding strategy can learn better representations for the attributed network clustering task.

The third group of baselines includes SDCN and NEC. Together with our proposed VCLANC, these methods aim to jointly learn the network embeddings and infer the clustering assignments for the attributed networks. As shown in Table 3 to Table 5, VCLANC outperforms SDCN and NEC on Cora, Citeseer and BlogCatalog. Take BlogCatalog dataset as an example, due to its increased network size and attributes number, the clustering performance of all the methods on BlogCatalog dataset decrease rapidly. Nevertheless, the NMI value and F1-score of the proposed method are 0.3036 and 0.4884, which still rank the best among all the methods. NEC and SDCN achieve similar results on NMI, ARI on BlogCatalog with the scores are around 0.27 and 0.19, respectively. But SDCN is much better than NEC and VCLANC on Flickr dataset in NMI, purity and ARI with the values as 0.2682, 0.3154 and 0.1665, respectively. The advantages of SDCN lies in its combined DNN and GCN structure, in which the DNN learns the overall information and GCN learns the local neighborhood structure. But it may be inconvenient as the DNN need to be pre-trained. At the same time, SDCN is more complicated than other methods as it requires much bigger neuron number in each layer (500-500-2000-10), while VCLANC and NEC only use a two-layer GCN (64-32).

Compared with SDCN, NEC uses the standard auto-encoder with soft clustering assignment loss and NEC also adopts extra modularity loss to exploit the higher-order proximity of nodes into the representation learning. However, NEC can not set different Gaussian priors to guide the embedding



(a) Raw attributes (b) GAE (c) VGAE (d) CAN

(e) SDCN (f) NEC (g) VCLANC

Figure 3. The t-SNE visualization for Cora dataset.

learning. On the contrary, VCLANC assumes a Gaussian mixture priors to guide the embedding learning of different node categories. Moreover, VCLANC also co-embeds the network and attribute into same semantic space to exploit the mutual affinities between nodes and attributes. Hence, VCLANC learns better node embeddings and outperforms NEC. What is more, when comparing CAN with VCLANC, the latter adopts GMM as priors for joint clustering purpose, which leads to better clustering performance. For example, the NMI of VCLANC is 0.5334 on Cora dataset while the NMI of CAN is 0.4893. As for the Citeseer dataset, VCLANC also show significant improvement over CAN with its ARI value as 0.407, which is higher than CAN with ARI as 0.3384. Therefore, it proves that joint learning the node embeddings and clustering assignments is useful when comparing the results of CAN and VCLANC.

6.2 Node Embedding Visualization

To qualitatively analyze the effectiveness of different methods in representation learning, we plot their node embeddings for

Table 7
Running time comparison (seconds).

Method	Cora	Citeseer	BlogCatalog	Flickr
GAE	7.73	26.91	79.20	167.10
VGAE	9.55	27.90	79.31	167.66
CAN	12.57	31.90	92.18	197.67
SDCN	35.26	42.90	124.66	198.12
NEC	19.02	39.89	105.25	220.45
VCLANC	17.75	36.33	97.76	204.48

Cora dataset into a 2-dimensional space using the popular dimension reduction tool: t-SNE [40]. Fig. 3 presents the visualization results from all the network embedding methods (Fig. 3 (b) to Fig. 3 (g)) and also the raw attributes of Cora dataset (Fig. 3 (a)). The color of the nodes represents their ground truth categories. As we can see in Fig. 3 (a), the raw attributes are not separable enough to distinguish different categorical nodes. Most nodes from different categories are mixed to each other. This drawback is eased by learning the low-dimensional embeddings for nodes. From Fig. 3 (b) to Fig. 3 (d), we show the embedding results of GAE, VGAE and CAN. As we can see, the categorical patterns could be easily noticed and the majority nodes from different categories of nodes are slightly separable to each other. But the boundary between different node groups are not clear. From Fig. 3 (e) to Fig. 3 (g), we show the embedding results of SDCN, NEC and VCLANC. We can see that SDCN does not show good separability for different clusters. But NEC and VCLANC have clear boundaries between the different categories. The red and brown categories of nodes are hard to be separated by NEC. But VCLANC has much pure clusters than NEC. For example, the yellow category of nodes is much pure and concentrated in Fig. 3 (g) than in Fig. 3 (f). Overall, our proposed method shows much better embedding effectiveness.

6.3 Running Time Comparison

We compare the efficiency of the graph neural network related methods over all the datasets. Each method is tested with 300 epochs for fair comparison. All the experiments are executed on an NVIDIA GPU with 11GB memory. As shown in Table 7, it is not surprised that GAE shows the least running time among all the methods since GAE only contains the basic encoder and decoder structure. For example, on cora dataset, GAE spends 7.73 seconds for running 300 epochs which is the lowest among all the methods. VGAE is slightly slower than GAE on other dataset as it involves an extra KL divergence loss and ranks as the second most efficient among all the methods. Its running time on Cora, Citeseer, BlogCatalog and Flickr is 9.55, 27.90, 79.31 and 167.66, respectively. Compared with VGAE, CAN is slower since it includes an extra VAE for embedding the attributes. The running time of CAN on Cora, Citeseer, BlogCatalog and Flickr is 12.57, 31.90, 92.18 and 197.67, respectively. Among SDCN, NEC and the proposed VCLANC, SDCN is the most inefficient on Cora, Citeseer and BlogCatalog datasets. This is because that SDCN adopts much deep graph neural network layers which brings more the parameters. But SDCN shows slighted better efficient than VCLANC on Flickr dataset. VCLANC is slightly worse in time consumption than CAN but far better than SDCN. For example, VCLANC spends 17.75 seconds on Cora dataset while SDCN requires 35.26 seconds and NEC requires 19.02 seconds. Overall, we can see that VCLANC is more efficient compared with NEC and SDCN for a self-contained clustering task.

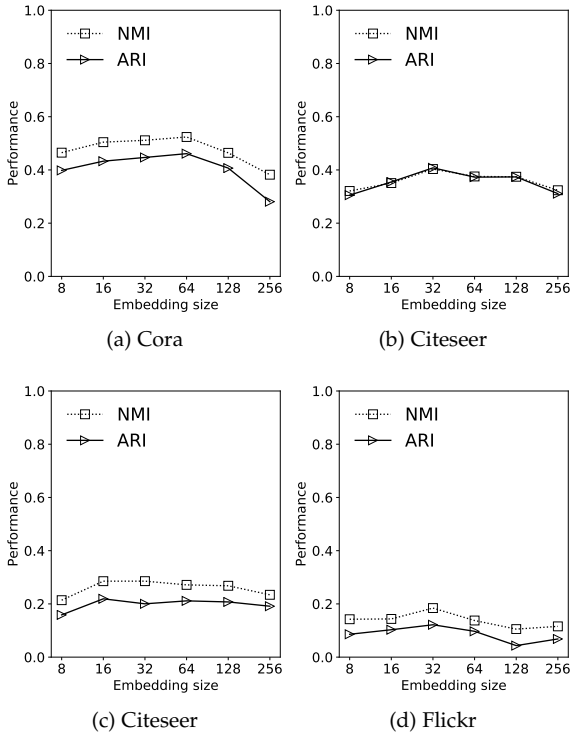


Figure 4. Embedding size analysis over all the datasets for the proposed method.

6.4 Embedding Size Analysis

In this section, we analyze the impacts of varying embedding size on the clustering performance for the proposed VCLANC. Fig. 4 shows the score trend of NMI and ARI by varying the embedding size. As we can see, when the embedding size is set as 32 or 64, VCLANC could achieve optimal performance on most of the datasets. Higher or lower embedding size may lead to the feature vectors become too sparse or uninformative to represent the best features for the vertices and thus leads to the decreasing of the clustering performance. The results indicate that VCLANC could learn informative node representations with relatively smaller embedding size.

7 Conclusions

In this paper, we have proposed a variational co-embedding learning model for attributed network clustering, called VCLANC. Compared with the other methods, VCLANC exploits dual variational auto-encoders to embed both nodes and attributes into the same latent space and reconstructs the mutual affinities between nodes and attributes as extra self-supervised knowledge for more distinguished embedding learning. At the same time, VCLANC adopts a trainable Gaussian mixture priors to infer the nodes clustering assignments in their embedding space. In this way, the network clustering process is not decoupled from the node representation learning process. On the contrary, the embedding space for the nodes could be optimized to find the best partitions for the networks. We have tested VCLANC on four real-world network datasets to validate its effectiveness. The experimental results show that

VCLANC outperforms the other methods in regard to different clustering metrics and learns better node representations based on the visualization analysis.

REFERENCES

[1] H. Cheng, Y. Zhou, and J. X. Yu, "Clustering large attributed graphs: A balance between structural and attribute similarities," *ACM Transactions on Knowledge Discovery from Data (TKDD)*, vol. 5, no. 2, pp. 1–33, 2011.

[2] M. Agrawal, M. Zitnik, J. Leskovec *et al.*, "Large-scale analysis of disease pathways in the human interactome." in *PSB*. World Scientific, 2018, pp. 111–122.

[3] D. Cao, X. He, L. Miao, G. Xiao, H. Chen, and J. Xu, "Social-enhanced attentive group recommendation," *IEEE Transactions on Knowledge and Data Engineering*, vol. 33, no. 3, pp. 1195–1209, 2021.

[4] Z. Xu, Y. Ke, Y. Wang, H. Cheng, and J. Cheng, "A model-based approach to attributed graph clustering," in *Proceedings of the 2012 ACM SIGMOD International Conference on Management of Data*, ser. SIGMOD '12. New York, NY, USA: Association for Computing Machinery, 2012, p. 505–516.

[5] H. Sun, F. He, J. Huang, Y. Sun, Y. Li, C. Wang, L. He, Z. Sun, and X. Jia, "Network embedding for community detection in attributed networks," *ACM Transactions on Knowledge Discovery from Data (TKDD)*, vol. 14, no. 3, pp. 1–25, 2020.

[6] D. Bo, X. Wang, C. Shi, M. Zhu, E. Lu, and P. Cui, "Structural deep clustering network," in *Proceedings of The Web Conference 2020*, ser. WWW '20. New York, NY, USA: Association for Computing Machinery, 2020, p. 1400–1410.

[7] C. Wang, S. Pan, R. Hu, G. Long, J. Jiang, and C. Zhang, "Attributed graph clustering: A deep attentional embedding approach," in *Proceedings of the Twenty-Eighth International Joint Conference on Artificial Intelligence 2019*, 2019, pp. 3670–3676.

[8] X. Zhang, H. Liu, Q. Li, and X.-M. Wu, "Attributed graph clustering via adaptive graph convolution," in *Proceedings of the Twenty-Eighth International Joint Conference on Artificial Intelligence 2019*, 2019, pp. 3670–3676.

[9] B. Perozzi, R. Al-Rfou, and S. Skiena, "Deepwalk: Online learning of social representations," in *Proceedings of the 20th ACM SIGKDD International Conference on Knowledge Discovery and Data Mining*, ser. KDD '14. New York, NY, USA: Association for Computing Machinery, 2014, p. 701–710.

[10] J. Tang, M. Qu, M. Wang, M. Zhang, J. Yan, and Q. Mei, "Line: Large-scale information network embedding," in *Proceedings of the 24th International Conference on World Wide Web*, ser. WWW '15. Republic and Canton of Geneva, CHE: International World Wide Web Conferences Steering Committee, 2015, p. 1067–1077.

[11] A. Grover and J. Leskovec, "Node2vec: Scalable feature learning for networks," in *Proceedings of the 22nd ACM SIGKDD International Conference on Knowledge Discovery and Data Mining*, ser. KDD '16. New York, NY, USA: Association for Computing Machinery, 2016, p. 855–864.

[12] L. F. Ribeiro, P. H. Saverese, and D. R. Figueiredo, "¡i¿struc2vec¡/i¿: Learning node representations from structural identity," in *Proceedings of the 23rd ACM SIGKDD International Conference on Knowledge Discovery and Data Mining*, ser. KDD '17. New York, NY, USA: Association for Computing Machinery, 2017, p. 385–394.

[13] T. N. Kipf and M. Welling, "Semi-supervised classification with graph convolutional networks," *arXiv preprint arXiv:1609.02907*, 2016.

[14] W. L. Hamilton, R. Ying, and J. Leskovec, "Inductive representation learning on large graphs," in *Proceedings of the 31st International Conference on Neural Information Processing Systems*, ser. NIPS'17. Red Hook, NY, USA: Curran Associates Inc., 2017, p. 1025–1035.

[15] S. Pan, R. Hu, G. Long, J. Jiang, L. Yao, and C. Zhang, "Adversarially regularized graph autoencoder for graph embedding," *arXiv preprint arXiv:1802.04407*, 2018.

[16] C. Wang, S. Pan, G. Long, X. Zhu, and J. Jiang, "Mgae: Marginalized graph autoencoder for graph clustering," in *Proceedings of the 2017 ACM on Conference on Information and Knowledge Management*, 2017, pp. 889–898.

[19] B. W. Kernighan and S. Lin, "An efficient heuristic procedure for partitioning graphs," *The Bell system technical journal*, vol. 49, no. 2, pp. 291–307, 1970.

[17] J. J. Choong, X. Liu, and T. Murata, "Learning Community Structure with Variational Autoencoder," *Proceedings - IEEE International Conference on Data Mining, ICDM*, vol. 2018-Novem, pp. 69–78, 2018.

[18] T. N. Kipf and M. Welling, "Variational graph auto-encoders," *arXiv preprint arXiv:1611.07308*, 2016.

[20] W. E. Donath and A. J. Hoffman, "Lower bounds for the partitioning of graphs," in *Selected Papers Of Alan J Hoffman: With Commentary*. World Scientific, 2003, pp. 437–442.

[21] J. Shi and J. Malik, "Normalized cuts and image segmentation," *IEEE Transactions on pattern analysis and machine intelligence*, vol. 22, no. 8, pp. 888–905, 2000.

[22] M. E. Newman, "Modularity and community structure in networks," *Proceedings of the national academy of sciences*, vol. 103, no. 23, pp. 8577–8582, 2006.

[23] R. Shang, J. Bai, L. Jiao, and C. Jin, "Community detection based on modularity and an improved genetic algorithm," *Physica A: Statistical Mechanics and its Applications*, vol. 392, no. 5, pp. 1215–1231, 2013.

[24] J. Yang and J. Leskovec, "Overlapping community detection at scale: A nonnegative matrix factorization approach," in *Proceedings of the Sixth ACM International Conference on Web Search and Data Mining*, ser. WSDM '13. New York, NY, USA: Association for Computing Machinery, 2013, p. 587–596.

[25] J. Neville, M. Adler, and D. Jensen, "Clustering relational data using attribute and link information," in *Proceedings of the text mining and link analysis workshop, 18th international joint conference on artificial intelligence*. Citeseer, 2003, pp. 9–15.

[26] D. R. Karger, "Global min-cuts in rnc, and other ramifications of a simple min-cut algorithm." in *SODA*, vol. 93. Citeseer, 1993, pp. 21–30.

[27] A. Y. Ng, M. I. Jordan, Y. Weiss *et al.*, "On spectral clustering: Analysis and an algorithm," *Advances in neural information processing systems*, vol. 2, pp. 849–856, 2002.

[28] Y. Zhou, H. Cheng, and J. X. Yu, "Clustering large attributed graphs: An efficient incremental approach," in *2010 IEEE International Conference on Data Mining*. IEEE, 2010, pp. 689–698.

[29] D. Combe, C. Largeron, E. Egyed-Zsigmond, and M. Géry, "Combining relations and text in scientific network clustering," in *2012 IEEE/ACM International Conference on Advances in Social Networks Analysis and Mining*. IEEE, 2012, pp. 1248–1253.

[30] D. P. Kingma and M. Welling, "Auto-encoding variational bayes," *arXiv preprint arXiv:1312.6114*, 2013.

[31] X. Li, Y. Hu, Y. Sun, J. Hu, J. Zhang, and M. Qu, "A deep graph structured clustering network," *IEEE Access*, vol. 8, pp. 161 727–161 738, 2020.

[32] Z. Jiang, Y. Zheng, H. Tan, B. Tang, and H. Zhou, "Variational deep embedding: an unsupervised and generative approach to clustering," in *Proceedings of the 26th International Joint Conference on Artificial Intelligence*, 2017, pp. 1965–1972.

[33] J. Xie, R. Girshick, and A. Farhadi, "Unsupervised deep embedding for clustering analysis," in *International conference on machine learning*. PMLR, 2016, pp. 478–487.

[34] J. MacQueen *et al.*, "Some methods for classification and analysis of multivariate observations," in *Proceedings of the fifth Berkeley symposium on mathematical statistics and probability*, vol. 1, no. 14. Oakland, CA, USA, 1967, pp. 281–297.

[35] Z. Meng, S. Liang, H. Bao, and X. Zhang, "Co-Embedding Attributed Networks," in *the Twelfth ACM International Conference*. New York, New York, USA: SIGIR, ACM Special Interest Group on Information Retrieval, jan 2019, pp. 393–401.

[36] D. P. Kingma and J. Ba, "Adam: A method for stochastic optimization," *arXiv preprint arXiv:1412.6980*, 2014.

[37] P. Sen, G. Namata, M. Bilgic, L. Getoor, B. Galligher, and T. Eliassi-Rad, "Collective classification in network data," *AI magazine*, vol. 29, no. 3, pp. 93–93, 2008.

[38] L. Tang and H. Liu, "Relational learning via latent social dimensions," in *Proceedings of the 15th ACM SIGKDD International Conference on Knowledge Discovery and Data Mining*, ser. KDD '09. New York, NY, USA: Association for Computing Machinery, 2009, p. 817–826.

[39] X. Huang, J. Li, and X. Hu, "Label informed attributed network embedding," in *Proceedings of the Tenth ACM International Conference on Web Search and Data Mining*, ser. WSDM '17. New York, NY, USA: Association for Computing Machinery, 2017, p. 731–739.

[40] L. van der Maaten and G. Hinton, "Visualizing data using t-sne," *Journal of Machine Learning Research*, vol. 9, no. 86, pp. 2579–2605, 2008.